TECHNICAL ARTICLE

Neutron diffraction studies of a double-crystal (+n,-m) setting containing a fully asymmetric diffraction geometry (FAD) of a bent perfect crystal (BPC)

P. Mikula,[1,a] M. Vrána,[1] J. Šaroun,[1] and V. Em[2]
[1]*Nuclear Physics Institute ASCR, v.v.i., 25068 Řež, Czech Republic*
[2]*National Research Centre "Kurchatov Institute", Moscow 123182, Russia*

(Received 11 August 2016; accepted 5 December 2016)

In this paper, some results of neutron diffraction properties of the double-crystal Si(111) + Si(311) setting containing two bent perfect crystals, but with the second one – analyzer in the fully asymmetric diffraction geometry are presented. Both fully asymmetric diffraction geometries, with the output beam compression as well as the output beam expansion, were tested for the sake of possible applications. © *2017 International Centre for Diffraction Data.* [doi:10.1017/S0885715616000725]

Key words: neutron diffraction, monochromator, bent perfect crystal, neutron optics

I. INTRODUCTION

Fully asymmetric diffraction (FAD) geometry is a limiting case of diffraction, which because of a rather large attenuation of X rays in a crystalline material can be practically used only with neutrons. Moreover, in order to avoid the primary and secondary extinction effect, the FAD geometry can be effectively exploited only in the case of homogeneously deformed perfect crystals with a small attenuation parameter covering also absorption. In fact, there are two possibilities of the FAD geometry: The geometry with the output beam compression (FAD-OBC) and the geometry with the output beam expansion (FAD-OBE). In the first case of the FAD-OBC geometry a wide neutron beam is impinging on the bent crystal and the diffracted beam passing along the longest edge of the crystal slab is formed in a narrow output beam [see Figure 1(a)]. On the other hand, in the latter case of the opposite FAD-OBE geometry, a narrow beam enters the bent-crystal slab (of the width of several millimeters) through its end face and after passing along the longest edge of the slab and depending on its curvature, the diffracted monochromatized beam can be expanded to a rather large cross-section [see Figure 1(b)]. The first attempts to study FAD geometry with Si bent perfect crystals were carried out in the eighties for a possible use as thermal neutron monochromators. The single-crystal FAD monochromators (Mikula *et al.*, 1986; Mikula *et al.*, 1987; Mikula *et al.*, 1990) as well as non-dispersive (1,–1) double-crystal arrangements (Mikula *et al.*, 1984; Mikula *et al.*, 1985; Mikula *et al.*, 1994) were studied and tested. These studies resulted in a design of a high-resolution double-crystal small-angle neutron scattering (SANS) diffractometer permitting the exploitation of 1d-PSD for collection of neutrons scattered by a SANS sample (Mikula *et al.*, 1988). The design has been realized in two instruments operating in NPI Rez as well as in HZ Berlin (Šaroun *et al.*, 1993; Šaroun *et al.*, 1994; Hempel *et al.*, 1996).

Recently, the attention has been focused on other FAD properties of the BPC slab, mainly in combination with other BPC slab of a different *d*-spacing in the so called parallel (+n,-m) double-crystal setting, which could provide further application possibilities. In this case the (+n,-m) setting can be considered as something between the dispersive and non-dispersive one. All the experiments were carried out in the three axis diffractometer mode when the double bent-crystal (+n,-m) setting was tested with the bent Si(111) premonochromator making some preselection of the monochromatic beam before passing through the (+n,-m) setting (Mikula *et al.*, 2014a, b). The obtained results provided favorable beam resolution properties with new application possibilities. The present paper also deals with the studies of the properties of the (+n,-m) setting; however, only in the double-axis mode (without a pre-monochromator) and different combination of the bent perfect crystals with a mutually larger difference in *d*-spacings. The properties of such performance have not been tested yet.

II. REFLECTING PROPERTIES OF A FAD-BPC SI SLAB

Generally, the BPC elements are attractive for employment because of the following reasons: predictability and reproducibility of the effective mosaicity, predictability, and reproducibility of a rather high peak reflectivity and its uniformity over large areas of the crystal, a rather high peak reflectivity for asymmetric or transmission geometry and predictability of the integrated reflectivity. When a neutron passing through the BPC crystal meets the Bragg condition it is reflected with the probability $r(R)$ (known often as a peak reflectivity), which is, of course, dependent on the bending radius R. For the FAD geometry the asymmetry cut angle $\psi = \pm\theta_0$ (θ_0 is the mean Bragg angle) $r(R)$ is equal for both cases (OBC as well as OBE). The peak reflectivity $r(R)$ has been derived for cylindrically BPC slab in a simple general form (Kulda, 1984; Mikula *et al.*, 1984)

$$r(R) = \left\{1 - \exp\left[-Q_{hkl}\left(\frac{\partial\Delta\theta}{\partial s_0}\right)^{-1}\right]\right\}, \qquad (1)$$

where $Q_{hkl} = (F_{hkl})^2 \cdot \lambda^3/(\Omega^2 \cdot \sin\ 2\theta_0)$ is the kinematical reflectivity of the crystal unit volume; F_{hkl}, λ and Ω are the

[a]Author to whom correspondence should be addressed. Electronic mail: mikula@ujf.cas.cz

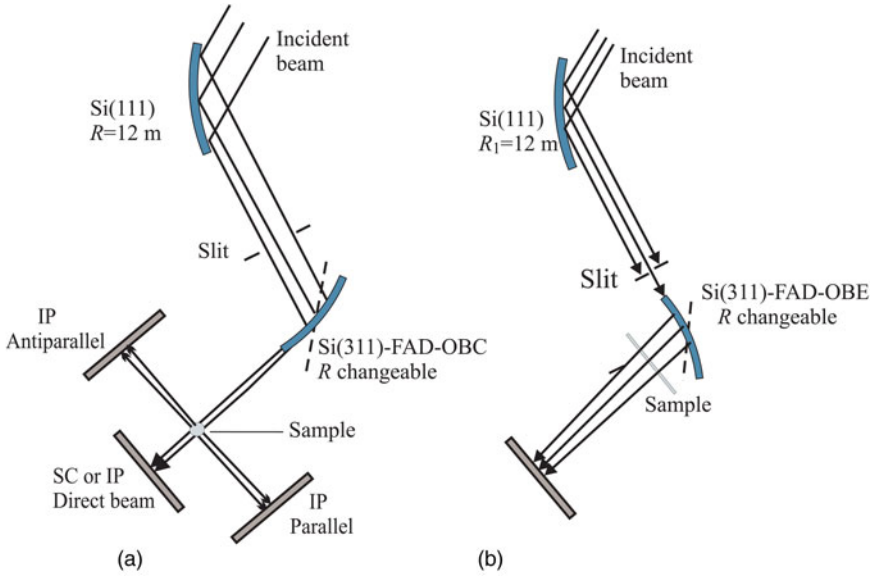

Figure 1. (Color online) Schematic view of the experimental performances using the FAD crystals in the OBC-diffraction geometry – (a) and OBE-diffraction geometry – (b). SC; scintillation counter; IP, imaging plate.

structure factor, neutron wavelength, and the unit-cell volume, respectively (Bacon, 1975). The rate of change of the Bragg angle on the flight path Δs_0 between the points A and B in the crystal (in the incident beam direction) is

$$\frac{\partial \Delta\theta}{\partial s_0} = \left(\frac{1}{R}\right)\left(\frac{\cos\psi}{\cos\theta_0}\right)[1-(1+\sigma)\sin(\theta_0+\psi)\sin(\theta_0-\psi)], \quad (2)$$

where σ is the Poisson constant. For the FAD geometry $\partial\Delta\theta/\partial s_0 = (1/R)$ and

$$r(R) = 1 - \exp(-Q_{hkl} \times R). \quad (3)$$

The difference $\delta\theta = \theta_1 - \theta_2$ (see Figure 2) is called effective mosaicity. It is clear that for the FAD-OBE geometry when $\psi = -\theta_0$ and the incident beam is passing along the longest edge of the BPC slab the effective mosaicity is $\delta\theta = l/R$ (l is the length of the slab) and can be very large. On the other hand, for FAD-OBC geometry when $\psi = +\theta_0$ the effective mosaicity is $\delta\theta = D/\sin 2\theta_0 / R$, where D is the thickness of the BPC slab. In both cases the effective mosaicity is proportional to BPC crystal curvature. Figure 3 shows the peak reflectivity dependences on the crystal curvature as calculated according to the formulae (1) and (3) for symmetric Si(111) and FAD (311) diffraction geometry, while the curve corresponding to the symmetric Si(311) diffraction geometry is introduced for the sake of comparison. Inspection of Figure 3 reveals that for small curvatures the peak reflectivity is equal to 1 as in the case of perfect crystal, but for stronger curvatures it decreases, being, however, still comparable or even larger than that of mosaic crystals.

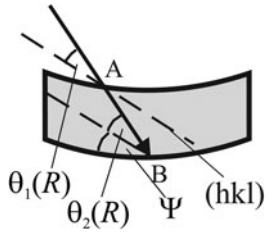

Figure 2. Detail of the incident beam passing through the BPC slab.

III. EXPERIMENTAL RESULTS

For this experiment, we used testing neutron optics diffractometer installed at the 10 MW medium power research reactor LWR-15. The diffractometer operates at the fixed neutron wavelength of $\lambda = 0.162$ nm, which is provided by a cylindrically bent perfect Si(111) crystal of the dimensions of $200 \times 40 \times 4$ mm^3 (length × width × thickness) and of the fixed radius of curvature of 12 m (see Figure 1). The second Si(311) crystal slab of the same dimensions as the first one was then used in two diffraction FAD-OBC as well as FAD-OBE geometries. No Soller collimators were used on the beam path from the reactor to the detector.

A. Double-crystal (+n,-m) arrangement: FAD-OBC geometry

First, the profiles of the output beam were measured by a scintillation camera (SC) at the distance of 50 cm from the

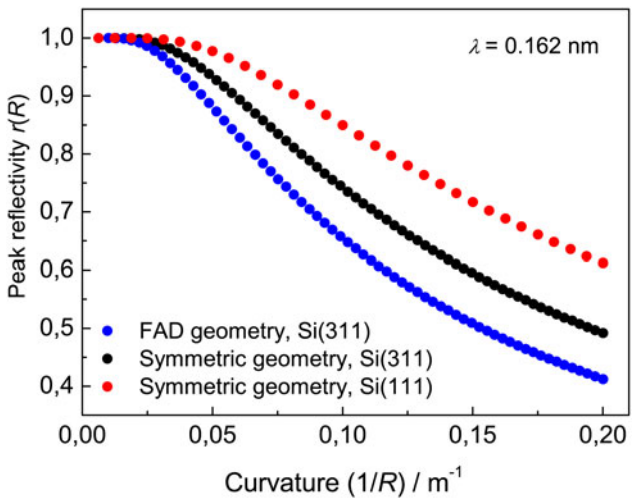

Figure 3. (Color online) The related peak reflectivities vs. crystal curvature as calculated according to the formulae (1) and (3).

https://doi.org/10.1017/S0885715616000725 Published online by Cambridge University Press

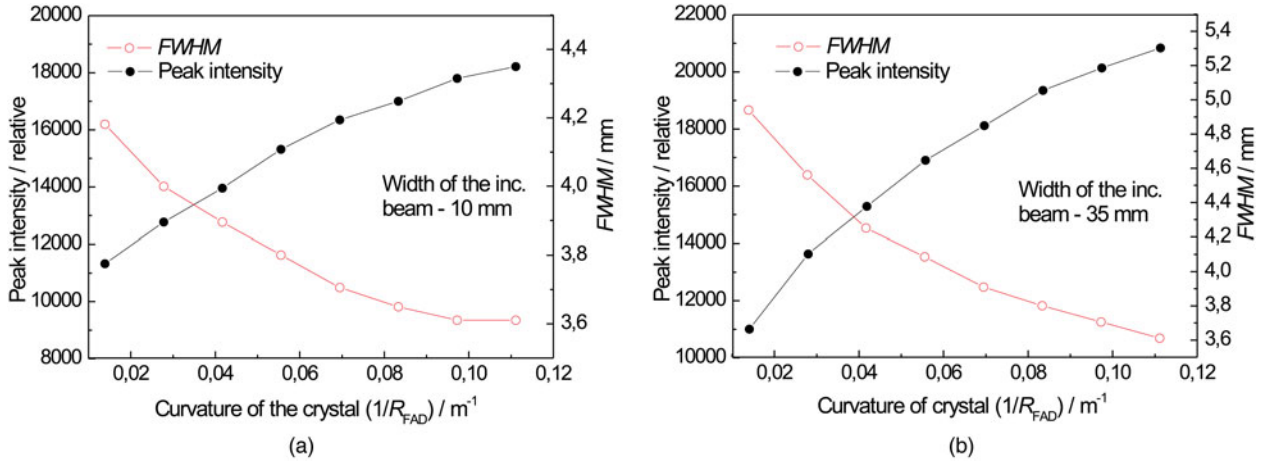

Figure 4. (Color online) Peak intensity and *FWHM* of the diffraction profile dependences on the FAD crystal curvature for a fixed curvature of the Si(111) one of 0.083 m^{-1} and for two widths of the incident beam of 10 mm – (a) and 35 mm – (b), respectively.

FAD crystal for its different curvatures and for two widths (made by a slit between the crystals) of the beam coming from the bent Si(111) slab on the FAD one. The obtained results are shown in Figure 4. It can be seen from Figure 4 that the width of the incident beam on the parameters of the double reflected output beam has little influence. It is brought about by the fact that the double-crystal (+n,-m) arrangement has a dispersive character and only neutrons within the beam width of about 10–15 mm are mostly reflected by the second FAD crystal. As expected, the Full Width at Half Maximum (FWHM) of the beam is determined by the thickness of the FAD crystal. For smaller curvatures, *FWHM* is still slightly influenced by the collimation of the beam between the crystals. As a second step, we put at the place of the third axis α-Fe polycrystalline pin of 2 mm diameter and measured the diffraction profiles by imaging plate (IP), at the distance of 45 cm from the pin [see Figure 1(a)]. This measurement was carried out in the so-called parallel as well as antiparallel geometry. Figure 5 shows examples of the obtained profiles for $R_{FAD} = 6$ m and the width of the slit for the beam incident on the FAD-crystal of 35 mm. It can be seen from Figure 5 that the obtained *FWHM*s are nearly equal. For the sake of comparison Figure 6 shows the equivalent profiles but for the slit width of 10 mm. Figure 7 summarizes the results of *FWHM*s (in mm) as registered by IP for different curvatures of the FAD crystal slab and for the width of the incident beam of 35 mm. It can be seen from Figure 7 that in the case of the maximum curvature (bending radius $R_{FAD} = 6$ m), *FWHMs* of the diffraction profiles for parallel and antiparallel geometry are nearly the same. In this way, it should be noticed that for the smaller width of the slit the resolution (determined by *FWHM*) was substantially improved. However, a small difference between the parallel and antiparallel geometry is still seen. If we take into account the distance of IP from the pin and its diameter, the estimation of the resolution of the diffracted beam from the α-Fe(211) pin expressed by the divergence $\Delta(2\theta_S)$ is about 6×10^{-3} rad for 35 mm slit and 1×10^{-3} or 2.5×10^{-3} for 10 mm slit and parallel or antiparallel geometry, respectively. It can be stated that in all cases a very high angular resolution was obtained. This property can be used namely in strain/stress measurements when two strain components can be measured simultaneously as it is used at the Time-of-Flight (TOF) stress instruments. Moreover, such high-resolution monochromatic beam can be

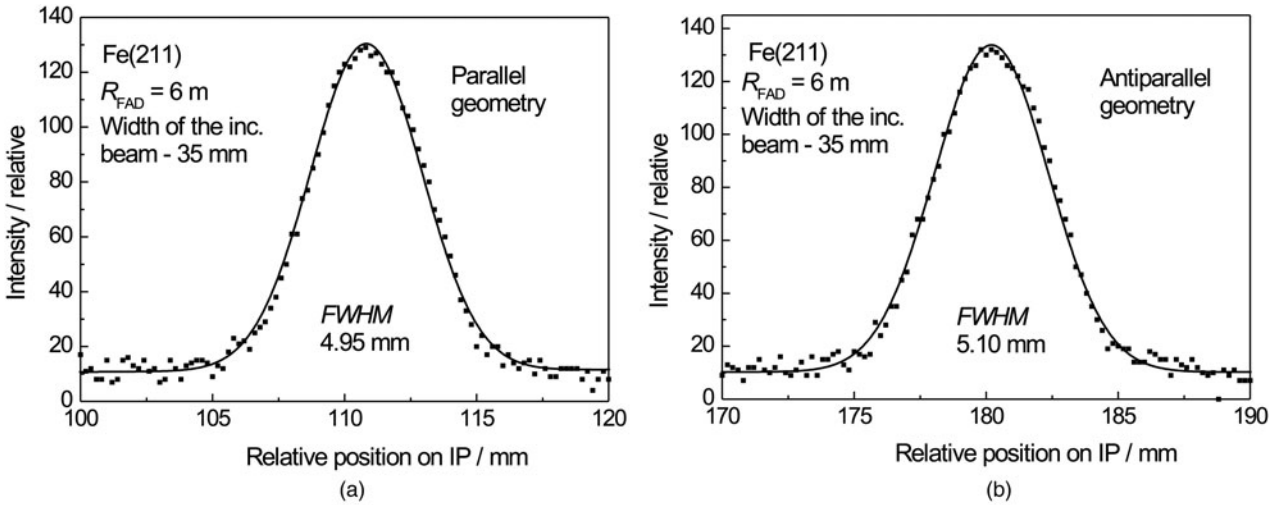

Figure 5. Diffraction profiles from the 2 mm α-Fe pin at the scattering angle of 88° and registered by IP at the distance of 45 cm for parallel – (a) and antiparallel – (b) scattering geometry and the width of the slit of 35 mm.

https://doi.org/10.1017/S0885715616000725 Published online by Cambridge University Press

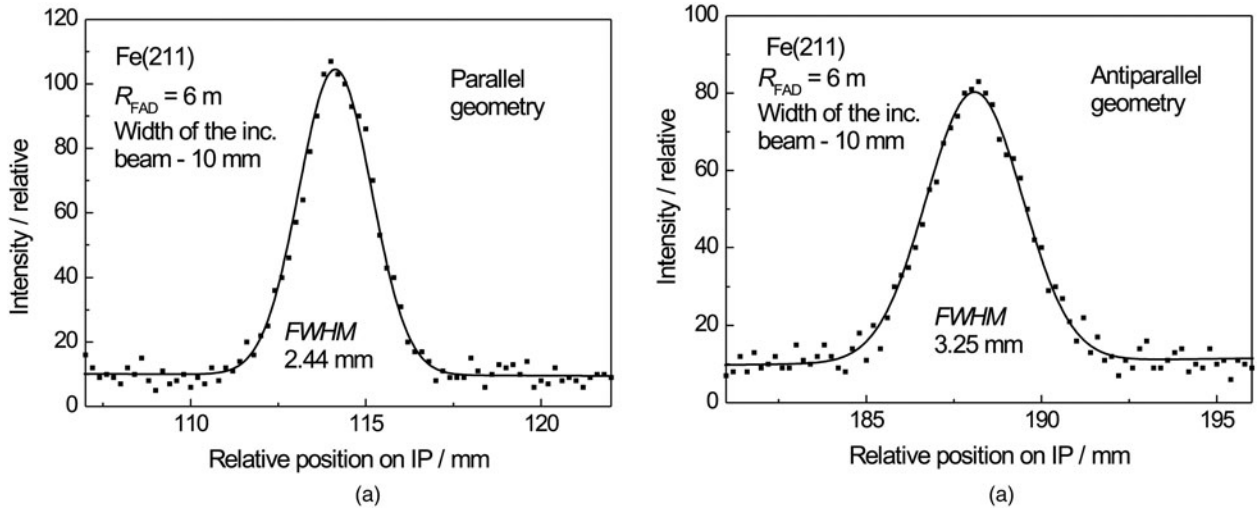

Figure 6. Diffraction profiles from the 2 mm α-Fe pin at the scattering angle of 88° and registered by the IP at the distance of 45 cm for parallel – (a) and antiparallel – (b) scattering geometry and the width of the slit of 10 mm.

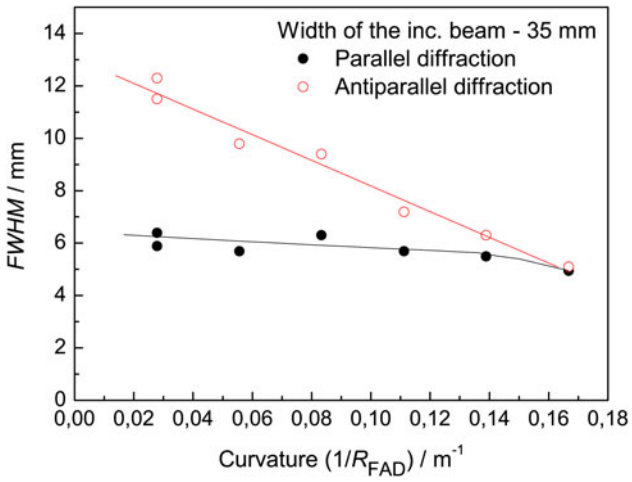

Figure 7. (Color online) *FWHM*s of the diffraction profiles from the 2 mm α-Fe(211) pin as registered by IP for different curvatures of the FAD crystal slab.

excellently used in studies of microstrains in polycrystalline materials from diffraction profile analysis, eventually, in diffraction experiments under an extreme load requiring samples of small dimensions.

B. Double-crystal (+n,-m) arrangement: FAD-OBE geometry

In this case, a narrow incident beam coming from the BPC Si(111) slab enters the FAD BPC Si(311) one through the end face and when neutrons passing the FAD slab along its longest edge meet the Bragg condition, they are reflected [see Figure 1 (b)]. Depending on the $\Delta\lambda$ and divergence of the incoming beam and the curvature of the FAD slab the area where all neutrons meet the Bragg condition inside the FAD slab can be large. Figure 8 shows the example of the image of the diffracted beam by the FAD crystal bent with $R_{FAD} = 12$ m. Some vertical shadows on the image are brought about by little attenuation of the Al-bars of the bending device. The larger the value of R_{FAD}, the longer the image of the beam can be

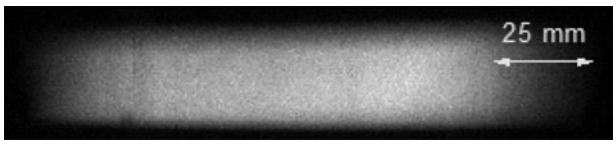

Figure 8. An example of the image of the diffracted beam by the FAD crystal for $R_{FAD} = 12$ m.

obtained. In the limiting case, the length of the image can be equal to the length of the FAD crystal slab. The height of the image is determined by the height of the slit (in our case it was 20 mm) which, of course, was lower than the height of the FAD crystal slab (in our case it was 40 mm). It is clear that by means of FAD-OBE geometry one can obtain a highly monochromatic and highly collimated beam of a large cross-section, which can be exploited, e.g. for neutron imaging. Figure 9 shows the image of the refraction effects observed at the edges of the individual rectangular teeth of a steel comb taken by the IP at the distance of 10 cm from the sample. The open space between the teeth is 2 mm and the period of the teeth is 6 mm. Similarly, Figures 10–12 show images of refraction effects on some other samples. It can be seen from these figures that the refraction contrast depends on the thickness of the sample (width of the edge face) as well as the coherent scattering amplitude of the material. All these refraction effect images document a high collimation property of the output diffracted beam.

IV. CONCLUSION

Inspection of Figures 4–6 reveals that contrary to a common view, the presented unconventional double-crystal monochromator exploiting the FAD-OBC analyzer in the (n,-m) quasi-dispersive setting can provide a sufficient neutron current at the sample position that can be used in powder diffractometry, of course, at a reasonably high flux neutron source. One should keep in mind that the quasi-dispersive setting behaves as a self-collimation assembly producing a highly monochromatized beam. By using such double-crystal monochromator, one can work with open beams without any Soller

https://doi.org/10.1017/S0885715616000725 Published online by Cambridge University Press

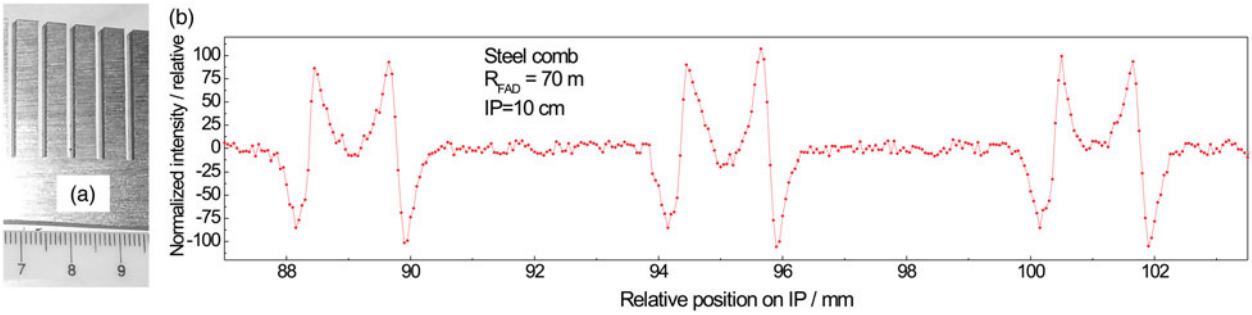

Figure 9. (Color online) Imaging of the refraction effects – (b) on the sample in the form of a steel comb – (a) with 4×4 mm^2 individual teeth.

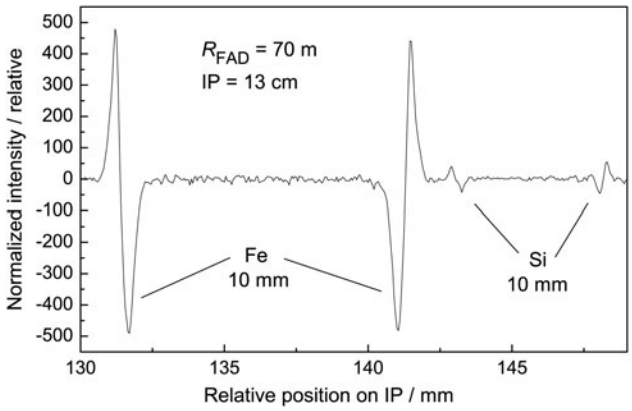

Figure 10. Imaging of the refraction effects on 10 mm-thick walls of the α-Fe and Si samples.

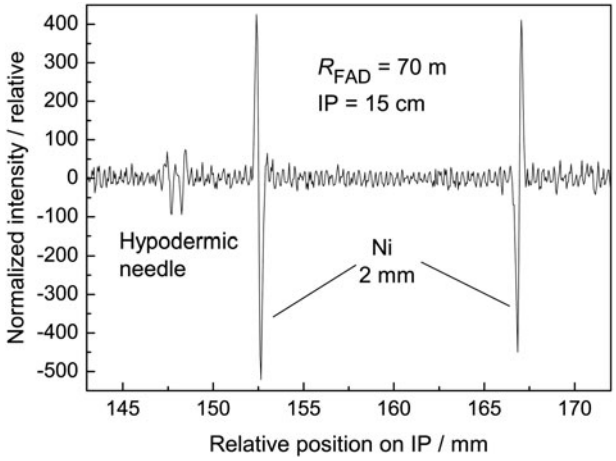

Figure 11. Imaging of the refraction effects on a hypodermic needle and 2 mm-thick walls of a Ni plate.

collimators. In the present case, it is necessary to point out that the instrument could not be fully optimized when using a fixed curvature of the Si(111) crystal. Furthermore, because of the given experimental conditions, the distance between the bent crystals was rather large (1.7 m). When all these parameters in connection with the possibility of using vertical focusing are optimally chosen, one can expect that the luminosity of the presented experimental setup could be one order of magnitude higher. By using a high-resolution position sensitive

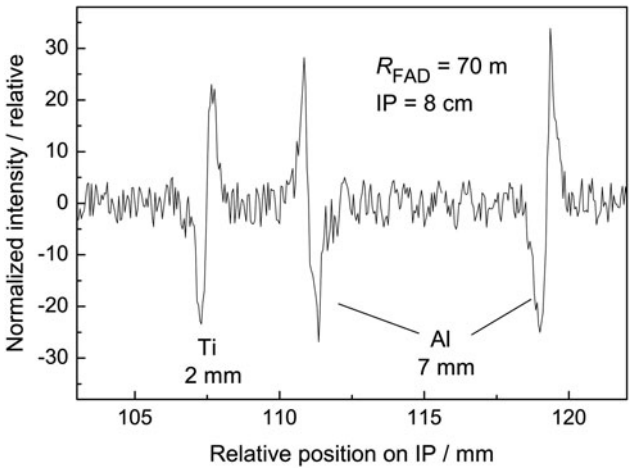

Figure 12. Imaging of the refraction effects on a 2 mm-thick Ti wall and a 7 mm-thick Al walls.

detector instead of IP having a rather low efficiency, the time expected for collection of the data related to individual diffraction profile is expected to be <20 min even at our medium power neutron source. For design and full optimization of such settings with the double bent-crystal monochromator [see Figure 1(a)], Monte Carlo simulations are desirable (Šaroun and Kulda, 2009).

As to the performance with the second crystal in the FAD-OBE geometry [see Figure 1(b)], one can obtain a highly collimated output beam of a large cross-section. It can be used for neutron imaging with a possibility of exploitation of the refraction effects on sample edges for increasing of the image contrast. However, because of the performance using neutron diffractometer, the high collimation beam and resolution are realized only in the scattering plane.

ACKNOWLEDGEMENTS

The related measurements were carried out at the CANAM infrastructure of the NPI ASCR Rez. Bragg diffraction optics investigations are, in the Czech Republic, supported by GACR project No. 16-08803J and by the ESS project LM2010011: “Contribution to Partnership in Large Research Infrastructure of Pan-European Importance”.

Bacon, C. G. (**1975**). *Neutron Diffraction* (Clarendon Press, Oxford). p. 67, 95.
Hempel, A., Eichhorn, F., Reichel, P., and Boede, W. (**1996**). “A neutron double-crystal diffractometer with a position sensitive detector for small-

https://doi.org/10.1017/S0885715616000725 Published online by Cambridge University Press

angle scattering studies", Nucl. Instrum. Methods Phys. Res. A **38**, 1466–1471.

Kulda, J. (**1984**). "A novel approach to dynamical neutron diffraction by a deformed crystal", Acta Crystallogr. A **40**, 120–126.

Mikula, P., Kulda, J., Vrána, M., and Chalupa, B. (**1984**). "A proposal of a highly efficient double crystal monochromator for thermal neutrons", J. Appl. Crystallogr. **17**, 189–195.

Mikula, P., Chalupa, B., Kulda, J., Vrána, M., Sedláková, L., and Michalec, R. (**1985**). "An experimental test of a double-crystal monochromator for thermal neutrons based on two bent silicon crystals", J. Appl. Crystallogr. **18**, 135–140.

Mikula, P., Kulda, J., Horalík, L., Chalupa, B., and Lukáš, P. (**1986**). "The Spatial condensation of the neutron beam by an asymmetric diffraction in thermal-neutron monochromatization", J. Appl. Crystallogr. **19**, 324–330.

Mikula, P., Lukáš, P., and Michalec, R. (**1987**). "An experimental test of a bent Si crystal as a thermal-neutron monochromator", J. Appl. Crystallogr. **20**, 428–430.

Mikula, P., Lukáš, P., and Eichhorn, F. (**1988**). "New version of a medium resolution double-crystal diffractometer for the study of a small angle neutron scattering (SANS)", J. Appl. Crystallogr. **21**, 33–37.

Mikula, P., Krüger, E., Scherm, R., and Wagner, V. (**1990**). "An elastically bent silicon crystal as a thermal neutron monochromator", J. Appl. Crystallogr. **23**, 105–110.

Mikula, P., Kulda, J., Lukáš, P., Vrána, M., and Wagner, V. (**1994**). "Bent perfect crystals in asymmetric diffraction geometry in neutron scattering experiments", Nucl. Instrum. Methods Phys. Res., Section A, **338**, 18–26.

Mikula, P., Vrána, M., Seong, B. S., Woo, W., Em, V., and Korytár, D. (**2014a**). "Neutron diffraction studies of a high resolution double crystal (+n,-m) setting containing Si(220) and Si(311) bent perfect crystals in symmetric and fully asymmetric diffraction geometry, respectively", IOP Publishing J. Phys. Conf. Ser. **528**, 012004.

Mikula, P., Vrána, M., Šaroun, J., Pilch, J., Seong, B. S., Woo, W., and Em, V. (**2014b**). "Neutron diffraction studies of double crystal (+n,-m) setting containing a fully asymmetric diffraction geometry (FAD) of a bent perfect crystal (BPC) with the output beam expansion (OBE)", J. Appl. Crystallogr. **47**, 599–605.

Šaroun, J. and Kulda, J. (**2009**). "Monte Carlo simulation package RESTRAX 5.2.0 and SIMRES 6.0.6", June 2009, http://neutron.ujf.cas.cz/restrax/index.php?chap=3/

Šaroun, J., Lukáš, P., Mikula, P., and Strunz, P. (**1993**). "Focusing doubly bent crystal diffractometer in combination with PSD for SANS experiments", J. Phys., Coll. C7, **3**, 439–442.

Šaroun, J., Lukáš, P., Mikula, P., and Alefeld, B. (**1994**). "Optimization of a double bent crystal diffractometer for neutron small angle neutron scattering experiments", J. Appl. Crystallogr. **27**, 80–88.

https://doi.org/10.1017/S0885715616000725 Published online by Cambridge University Press